DNA interactions and biological activity of 2,9-disubstituted 1,10-phenanthroline thiosemicarbazone-based ligands and a 4-phenylthiazole derivative

Álvaro Nicolás,[a,b] Julia G. Quero,[a] Marta Barroso,[a] Zoila Gándara,[a,b*] and Lourdes Gude[a,b*]

[a]*Universidad de Alcalá, Departamento de Química Orgánica y Química Inorgánica, Instituto de Investigación Química "Andrés M. del Río" (IQAR), 28805-Alcalá de Henares, Madrid, Spain.*
[b]*Grupo DISCOBAC, Instituto de Investigación Sanitaria de Castilla-La Mancha (IDISCAM), Spain.*

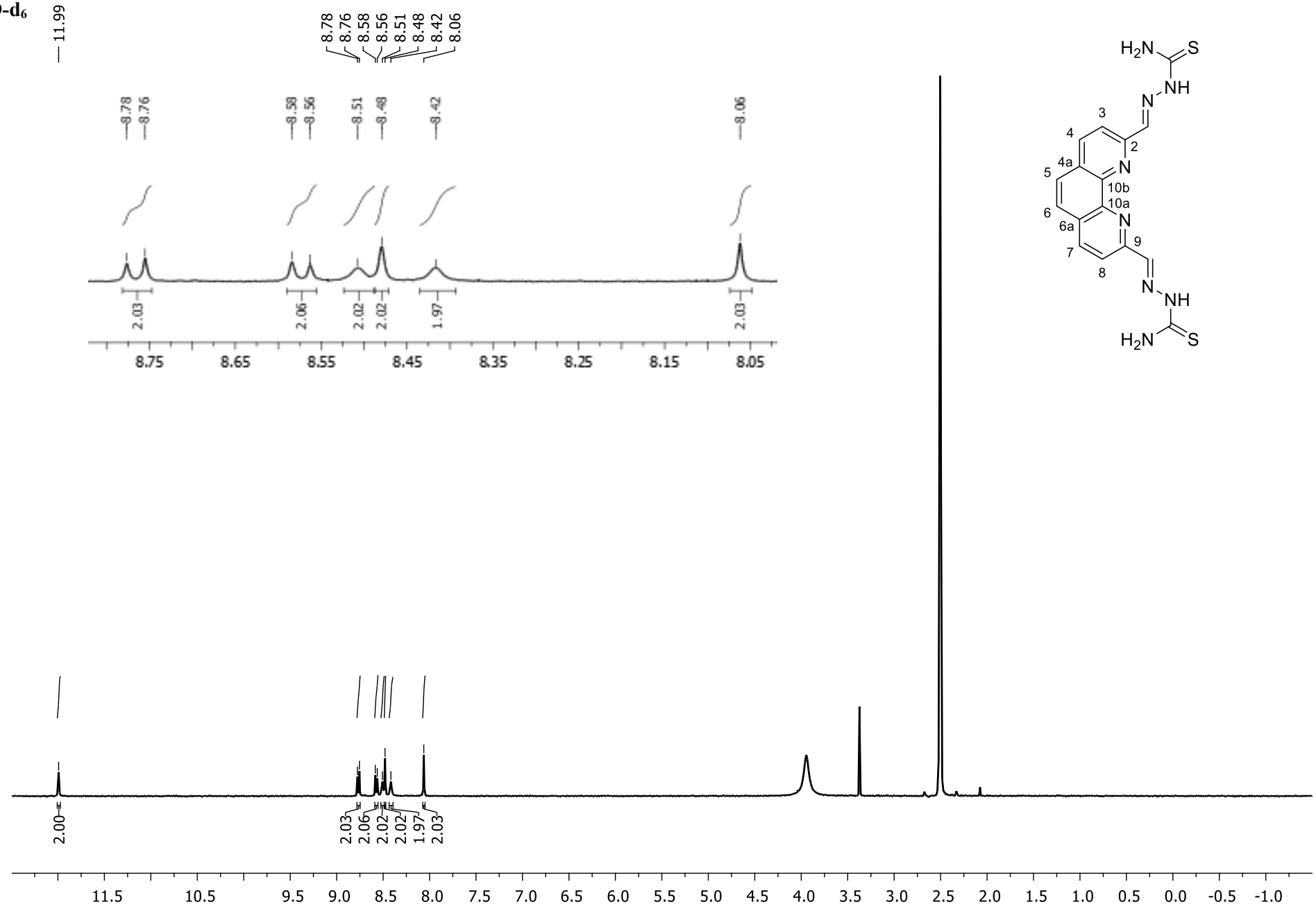

Figure S1. ^{1}H NMR (400 MHz, DMSO-d$_6$) of **1**

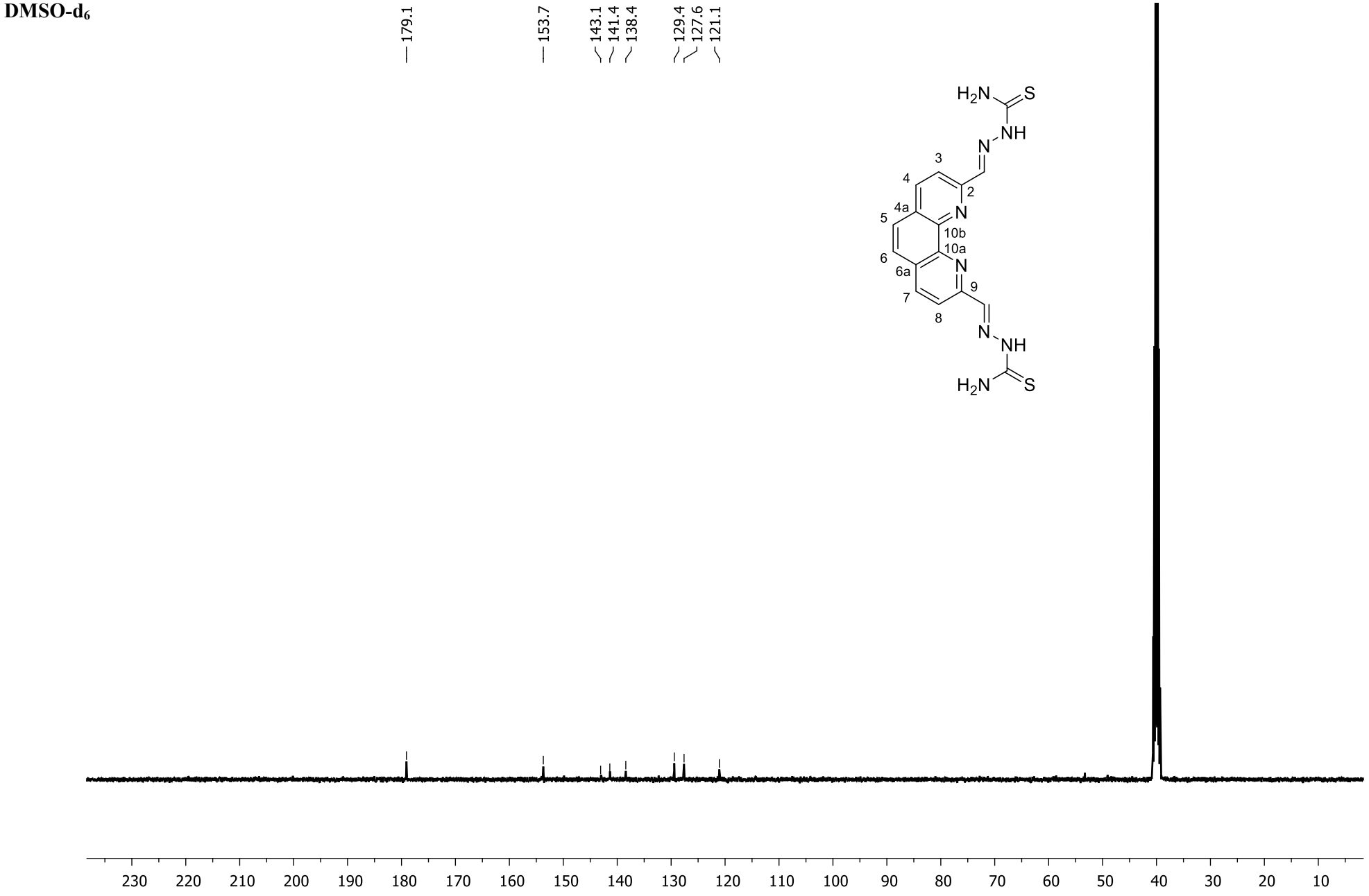

Figure S2. ^{13}C NMR (101 MHz, DMSO-d6) of **1**

DMSO-d$_6$

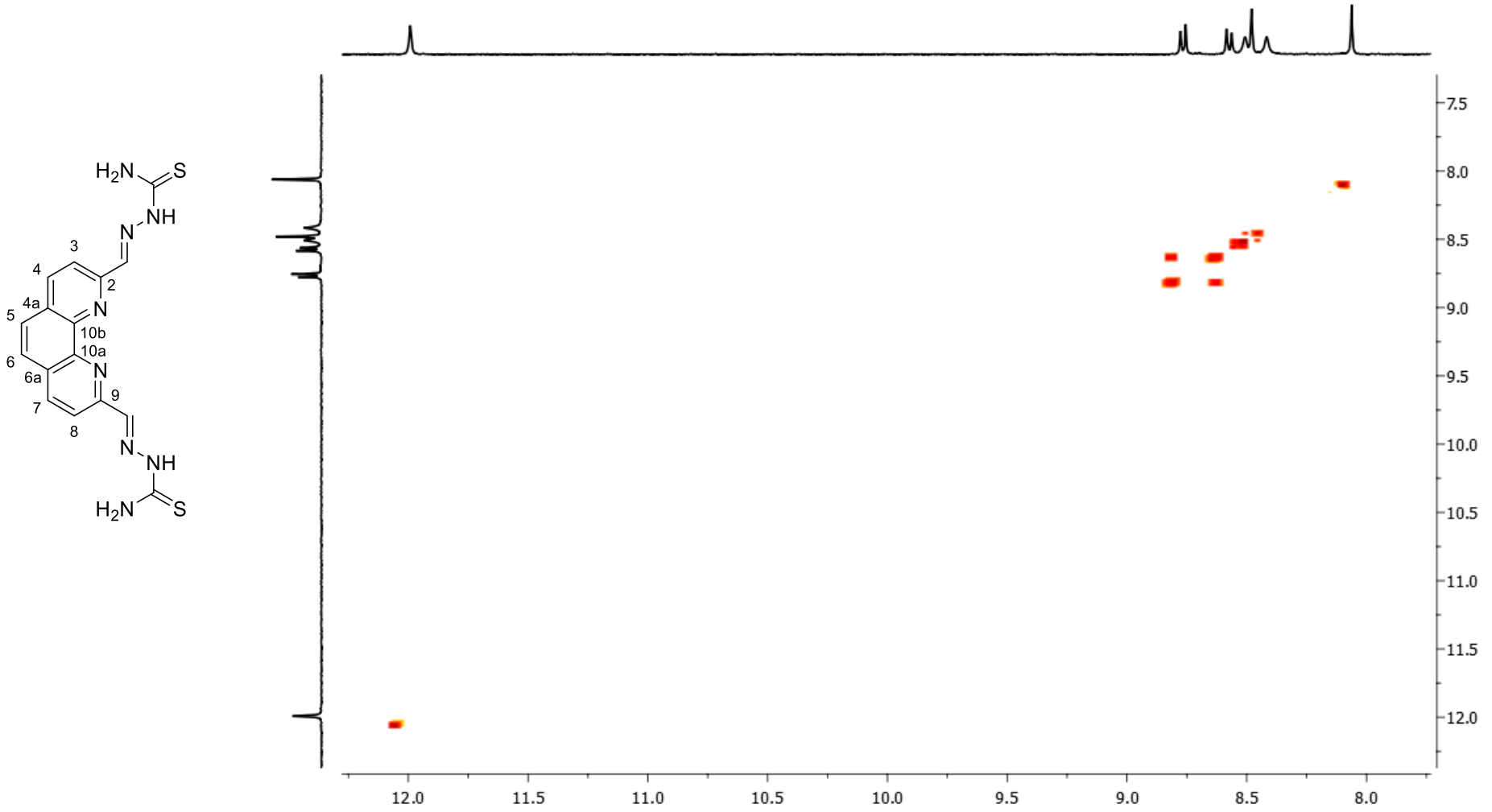

Figure S3. ^{1}H-^{1}H-COSY (400 MHz, DMSO-d6) of **1**

DMSO-d$_6$

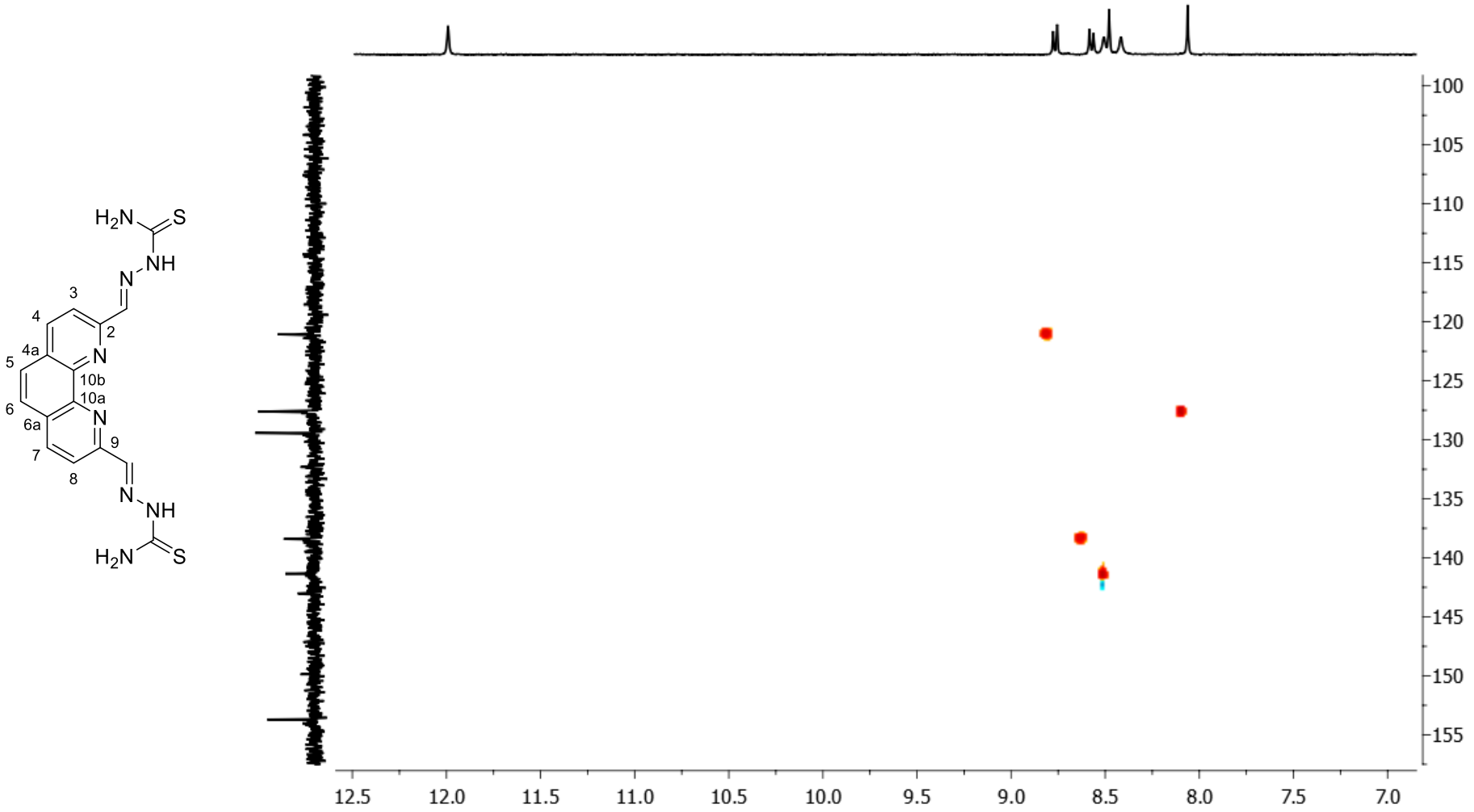

Figure S4. ^{1}H-^{13}C-HSQC (400 MHz, DMSO-d6) of **1**

DMSO-d$_6$

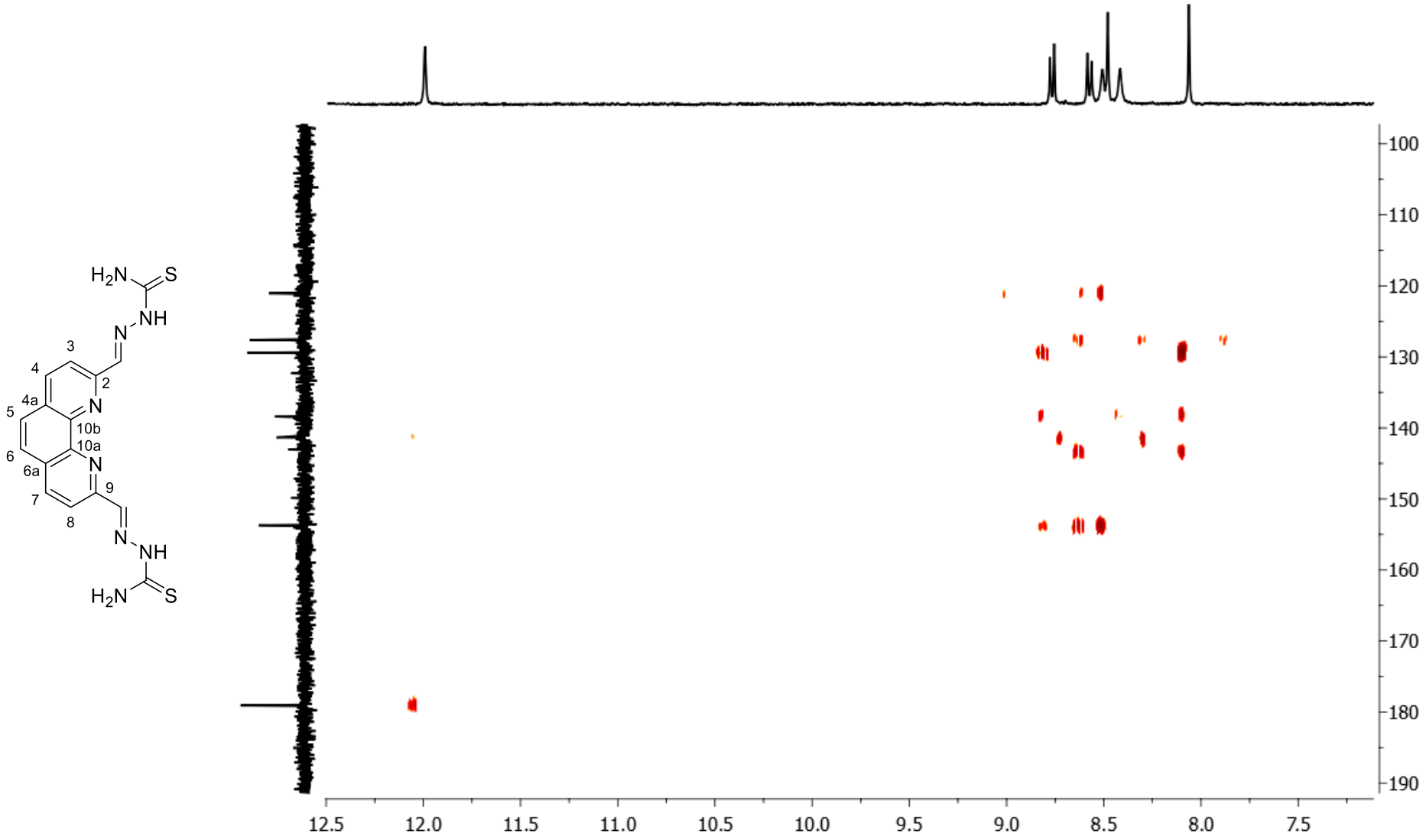

Figure S5. ^{1}H-^{13}C-HMBC (400 MHz, DMSO-d6) of **1**

DMSO-d_6

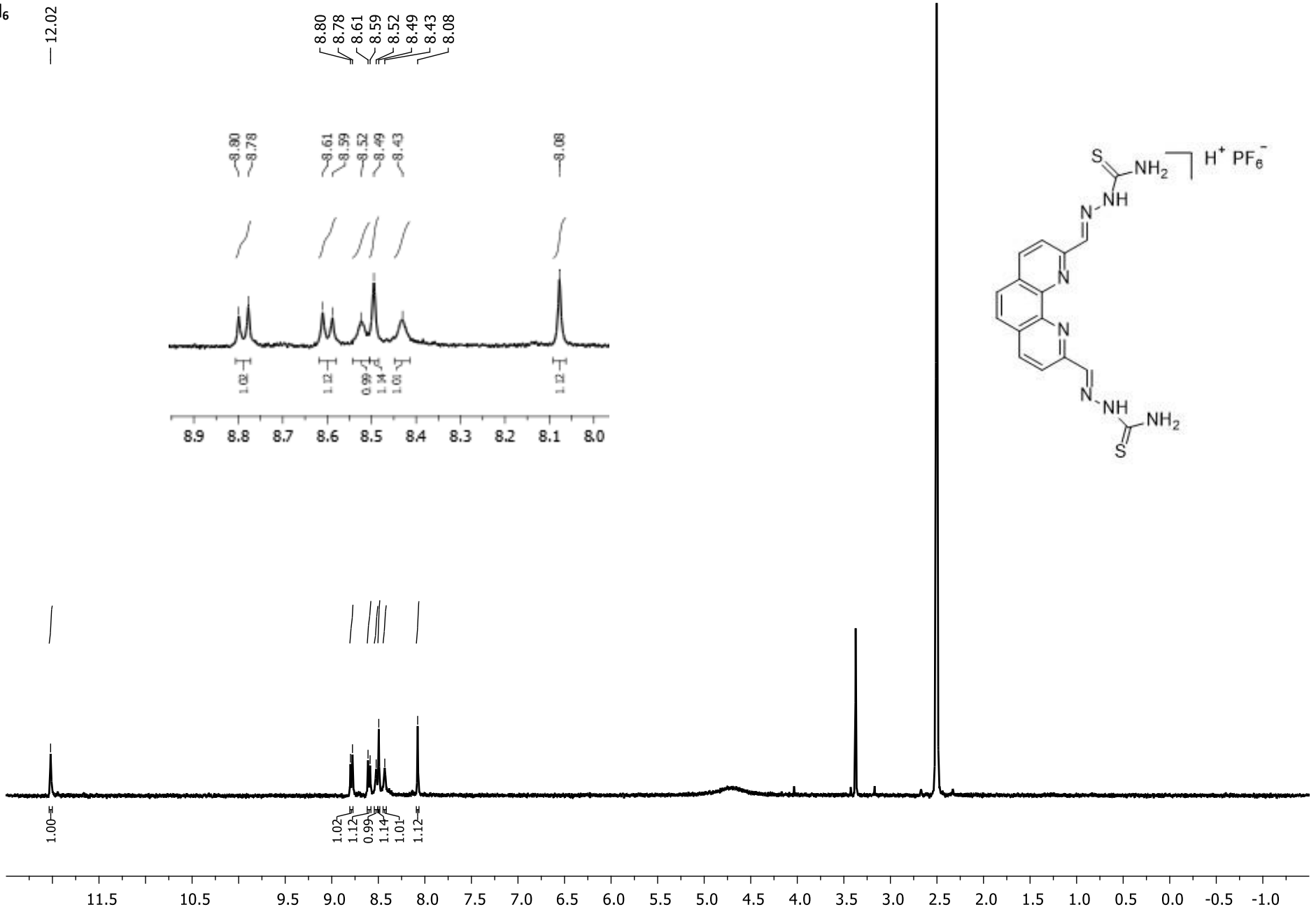

Figure S6. ^{1}H NMR (400 MHz, DMSO-d_6) of **2**

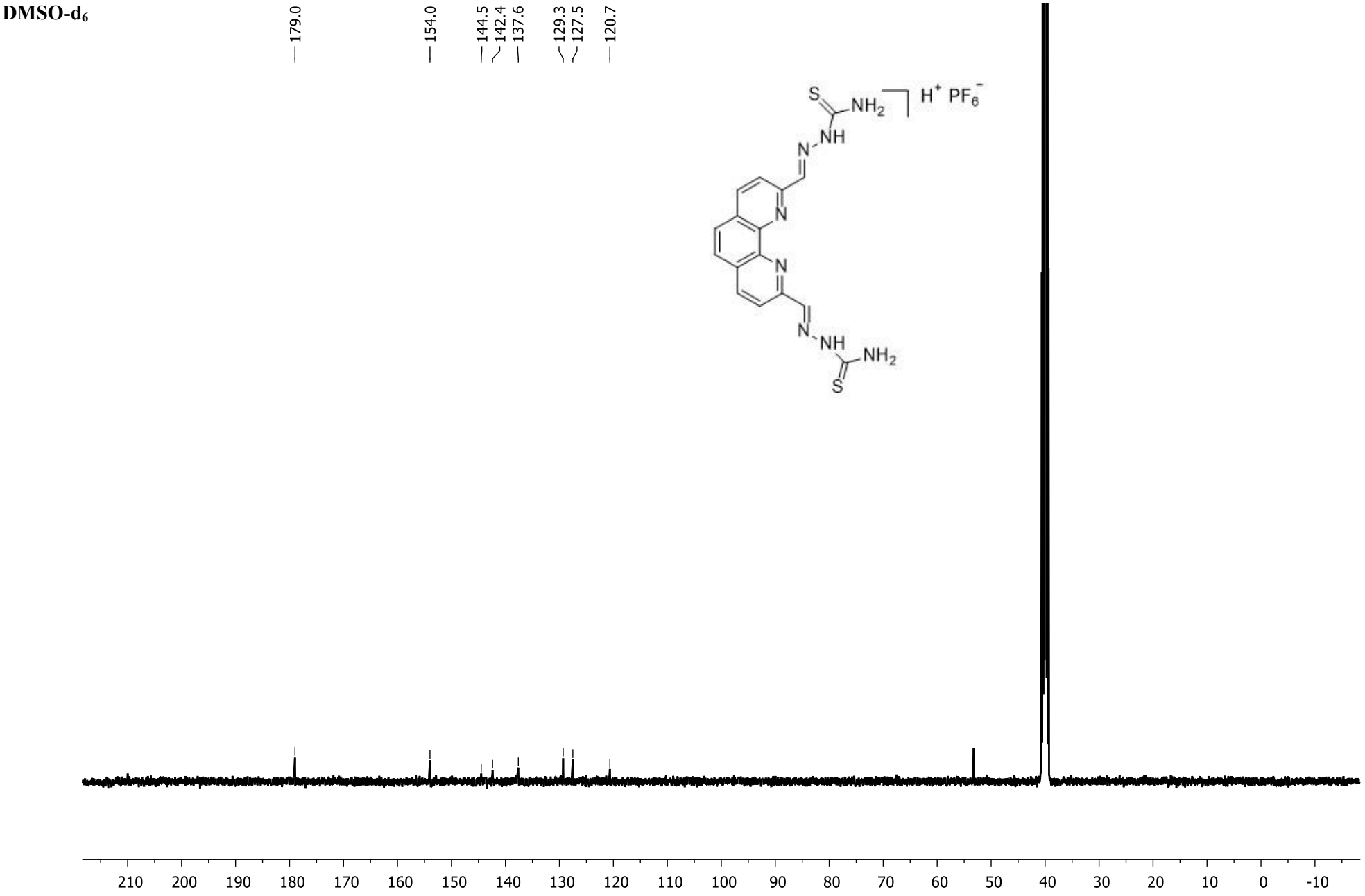

Figure S7. ^{13}C NMR (101 MHz, DMSO-d$_6$) of **2**

DMSO-d$_6$

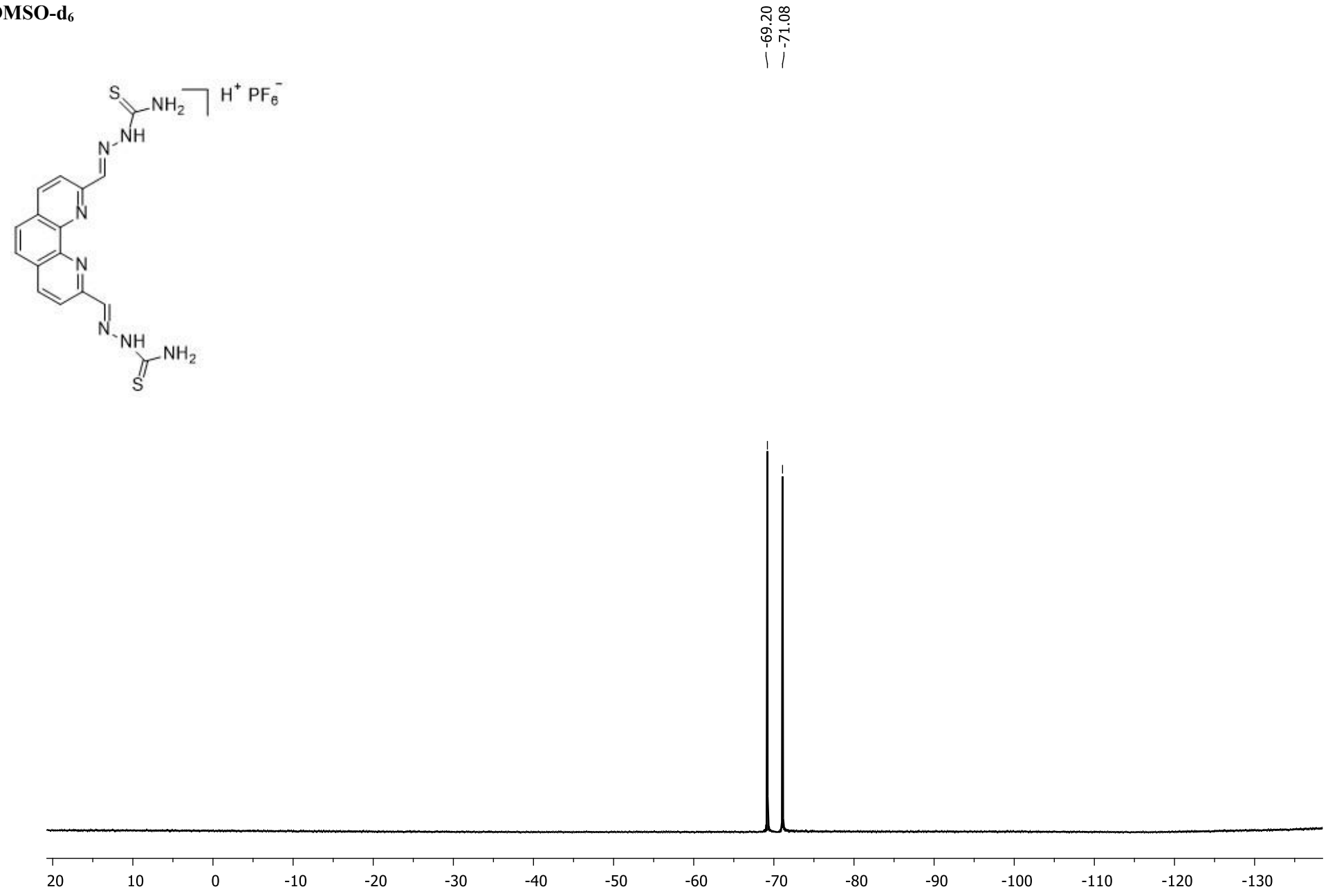

Figure S8. ^{19}F NMR (376 MHz, DMSO-d$_6$) of **2**

DMSO-d$_6$

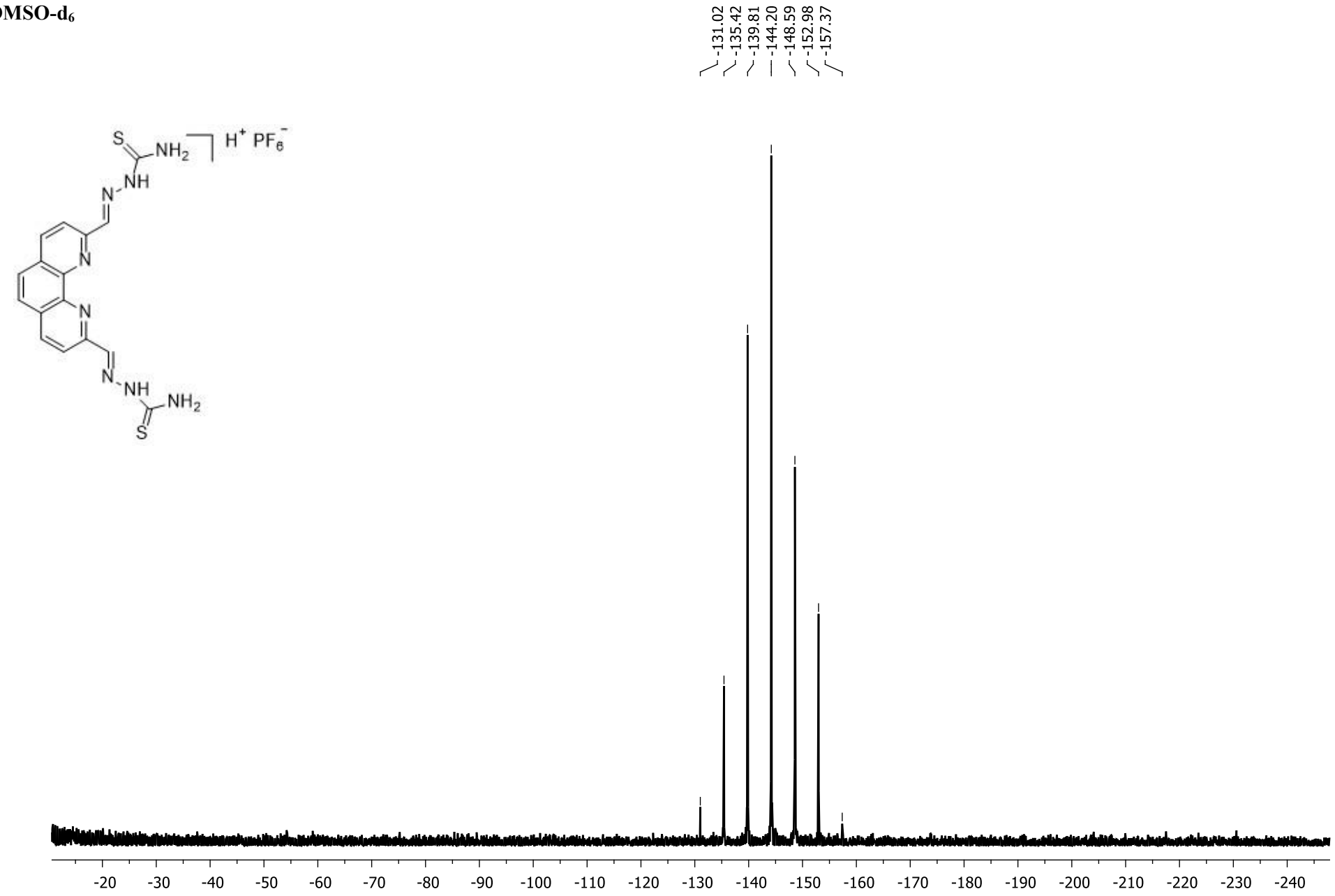

Figure S9. ^{31}P NMR (162 MHz, DMSO-d$_6$) of **2**

DMSO-d$_6$

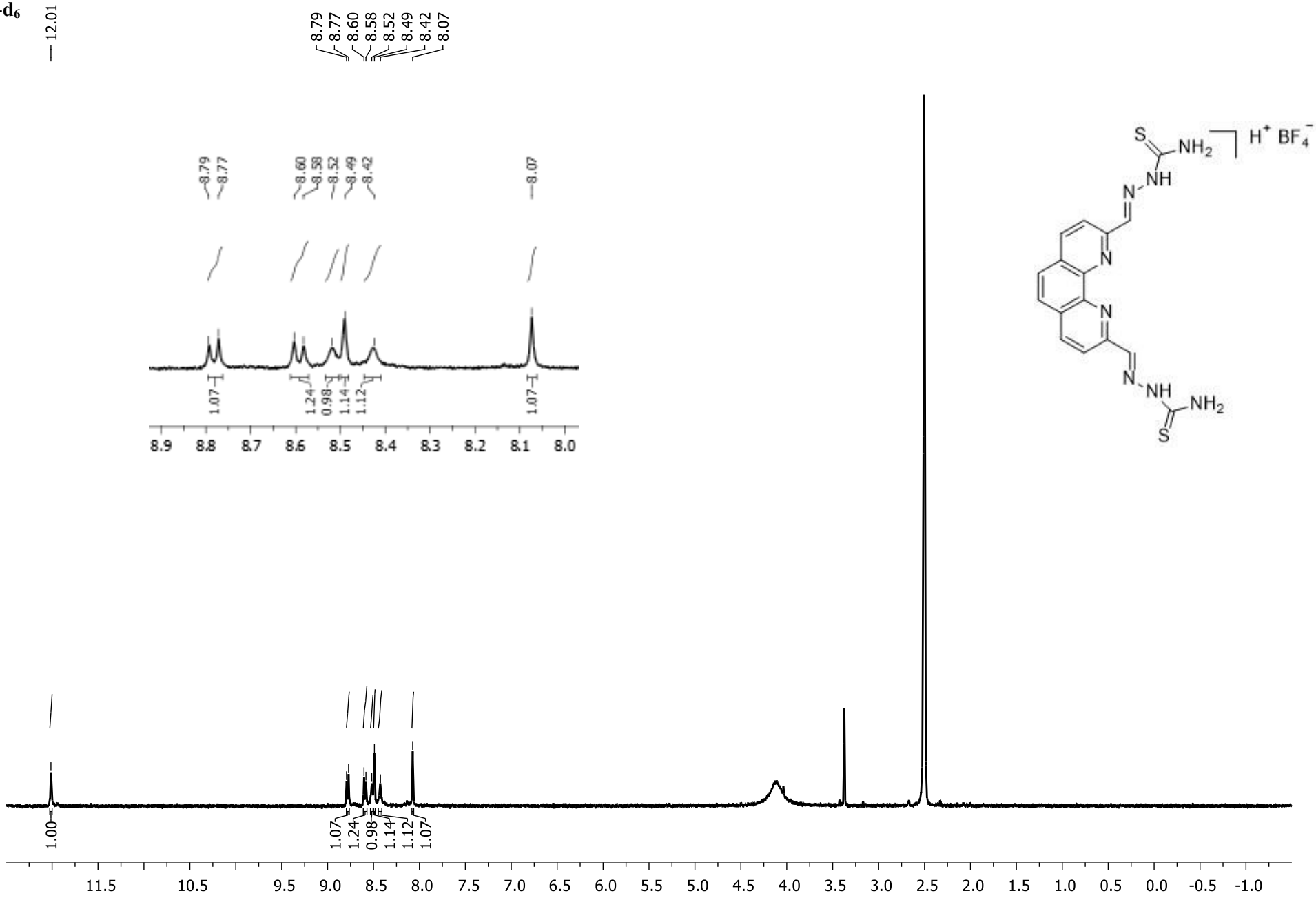

Figure S10. ^{1}H NMR (400 MHz, DMSO-d$_6$) of **3**

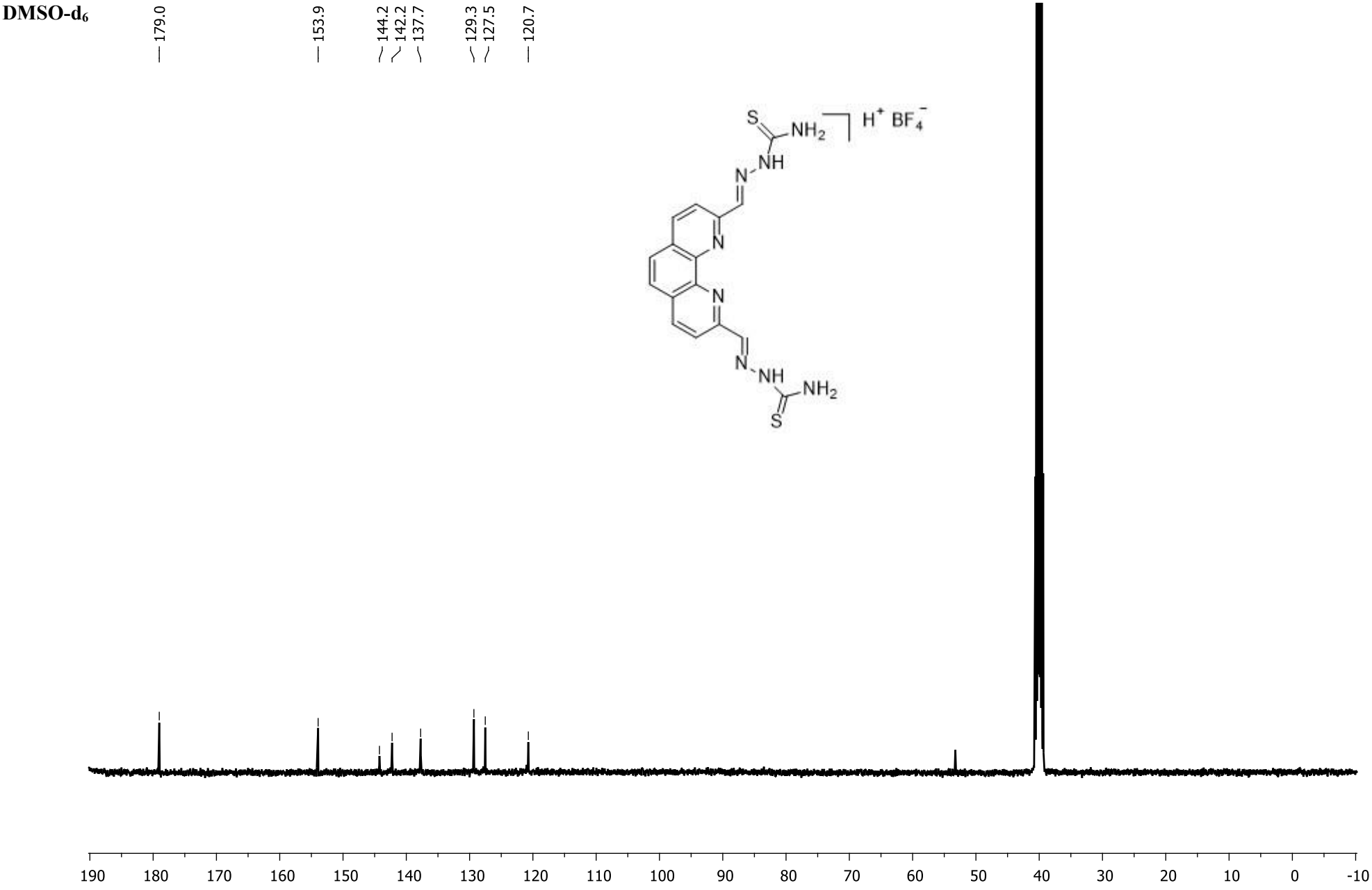

Figure S11. ^{13}C NMR (101 MHz, DMSO-d_6) of **3**

DMSO-d$_6$

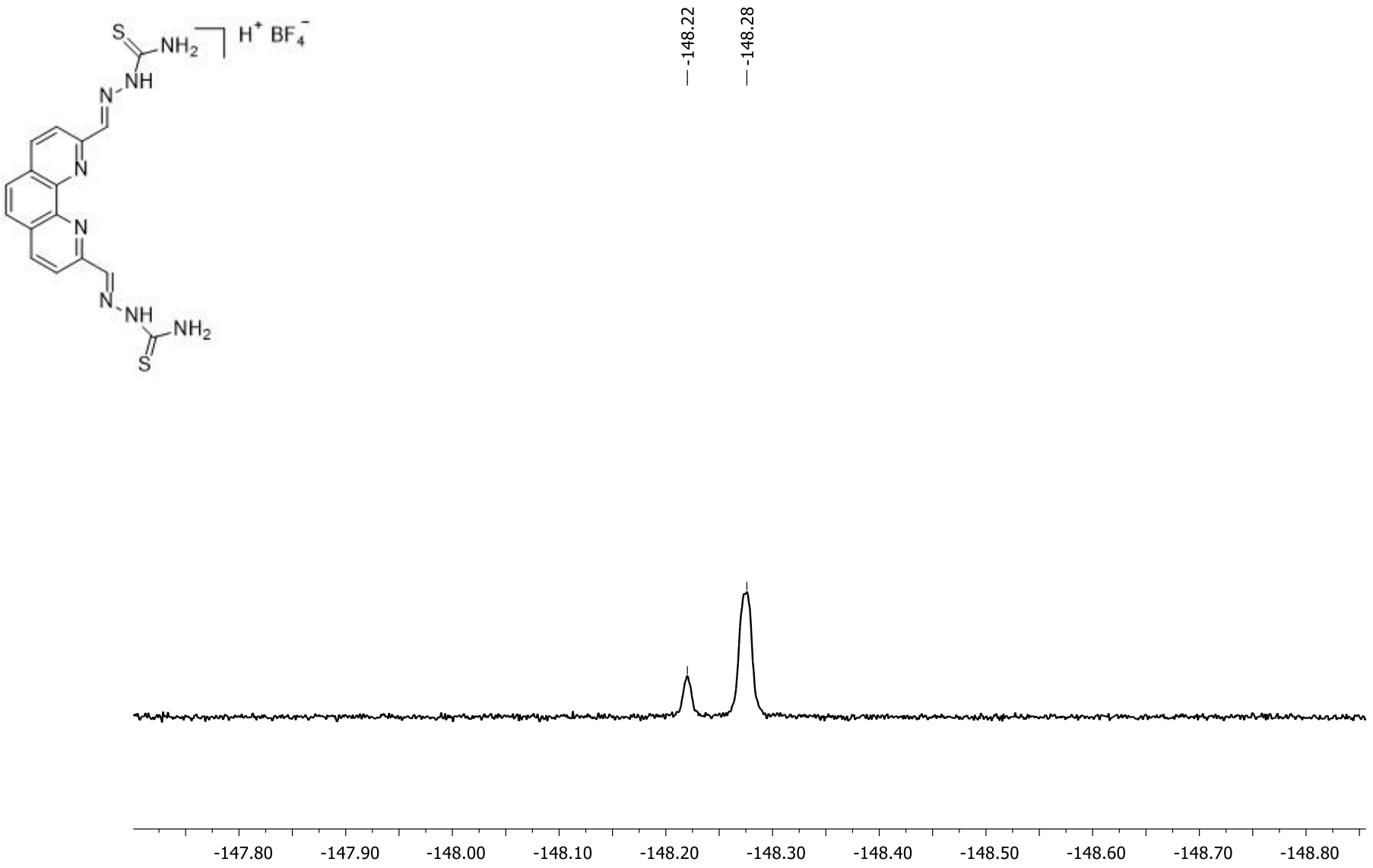

Figure S12. ^{19}F NMR ((376 MHz, DMSO-d$_6$) of **3**

DMSO-d_6

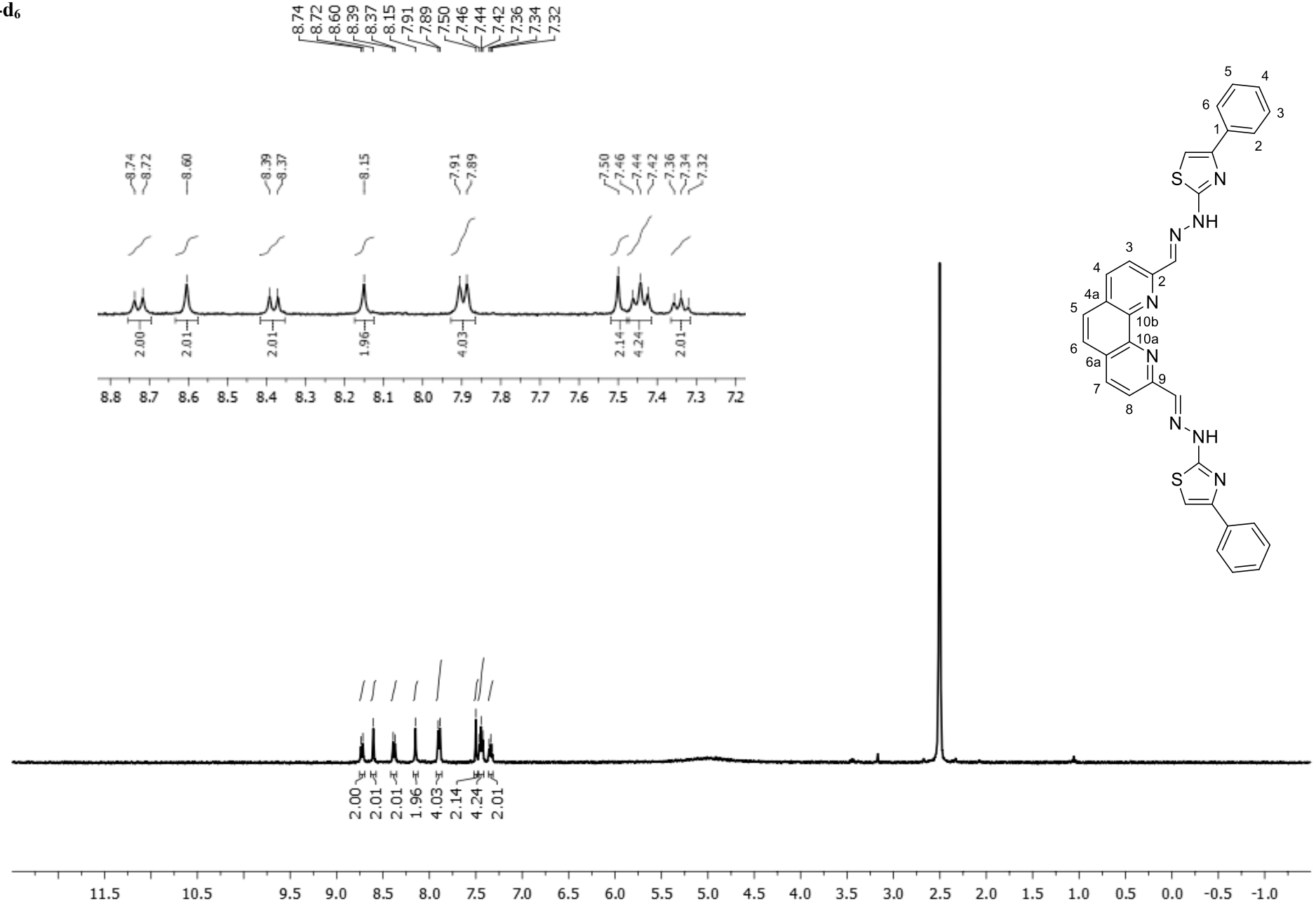

Figure S13. ^{1}H NMR (400 MHz, DMSO-d_6) of **4**

DMSO-d_6

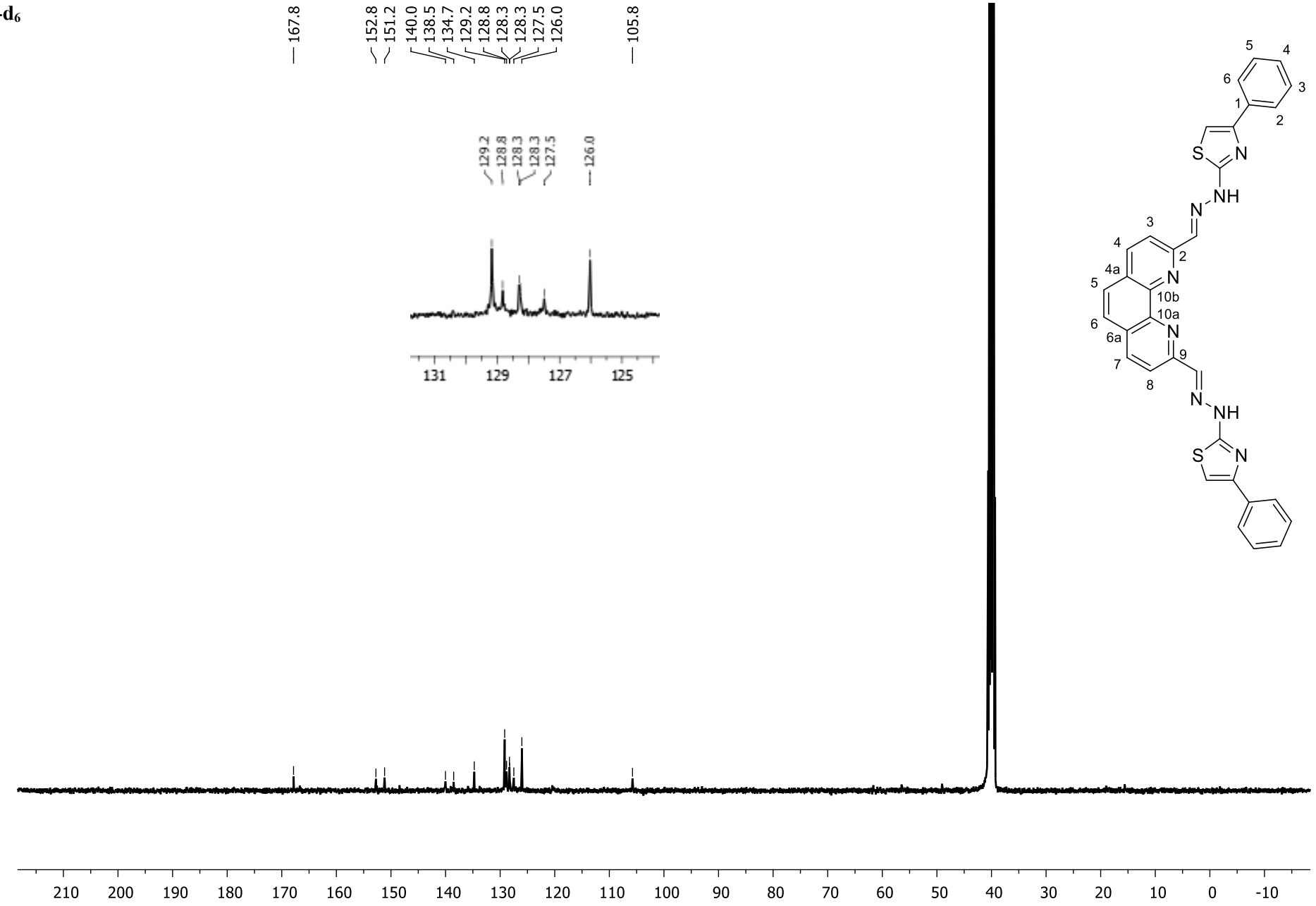

Figure S14. ^{13}C NMR (101 MHz, DMSO-d_6) of **4**

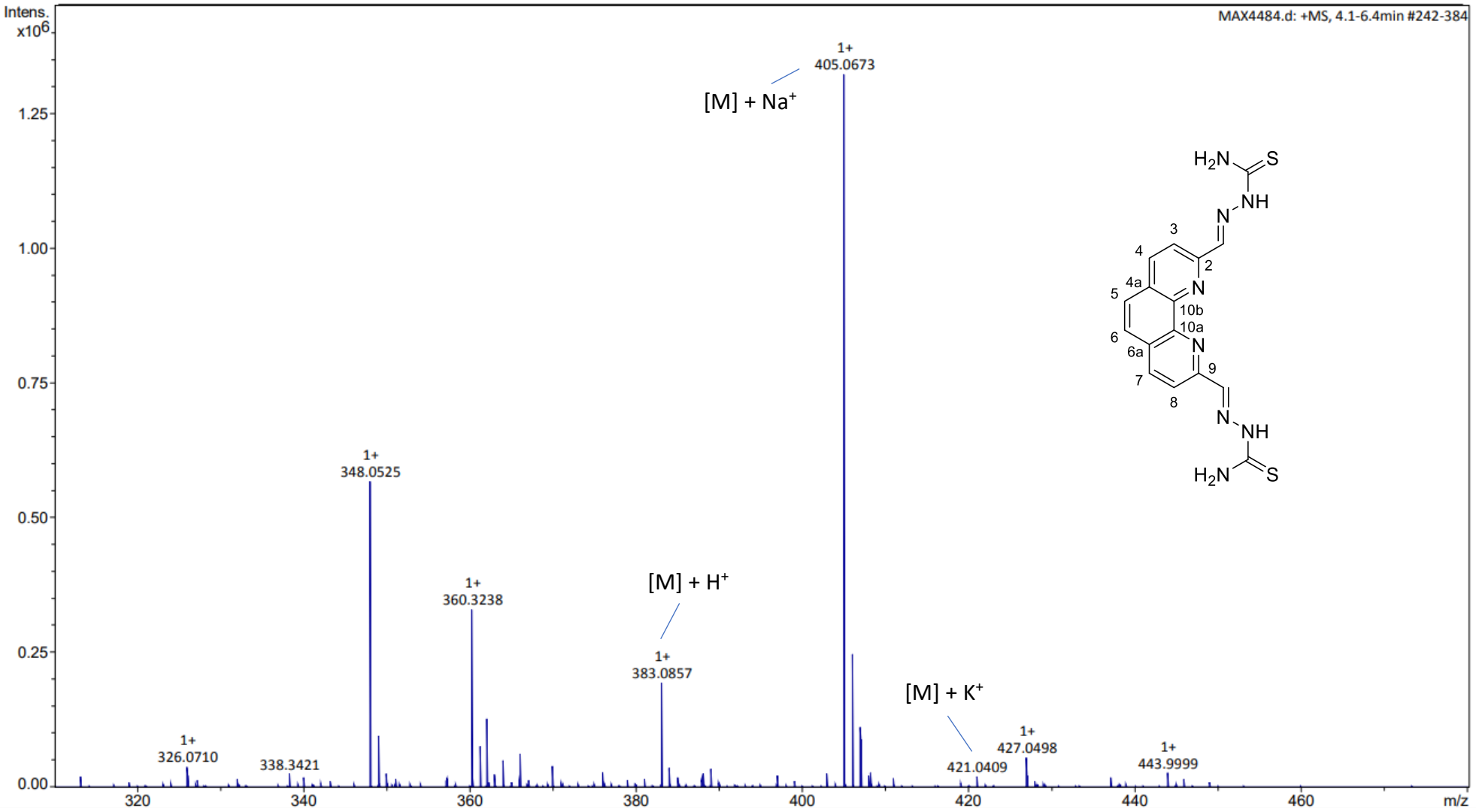

Figure S15. Zoomed view of high-resolution electrospray ionization mass spectrum (ESI-HRMS-pos) of **1** (MeOH, 1% formic acid)

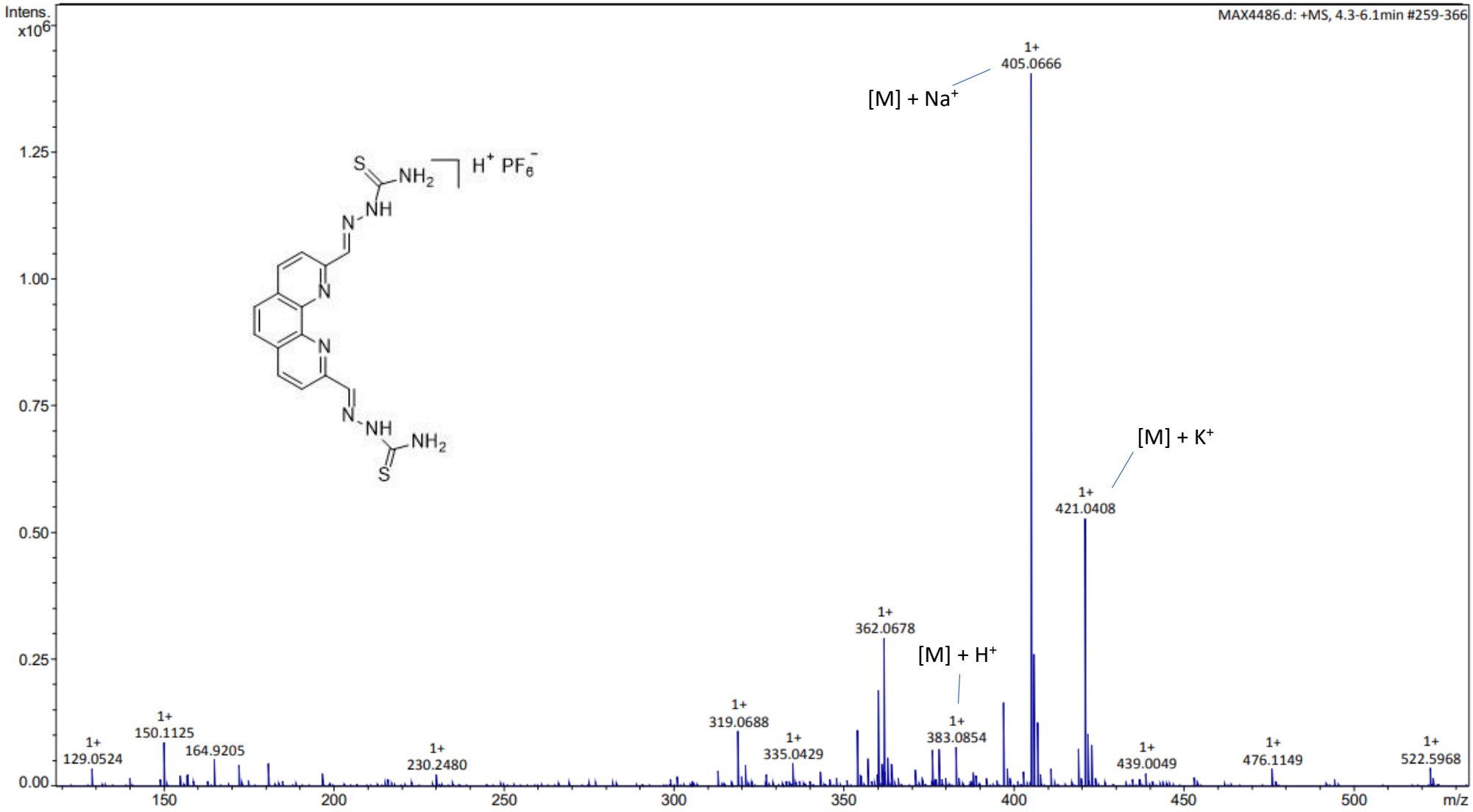

Figure S16. Zoomed view of high-resolution electrospray ionization mass spectrum (ESI-HRMS-pos) of **2** (MeOH, 1% formic acic)

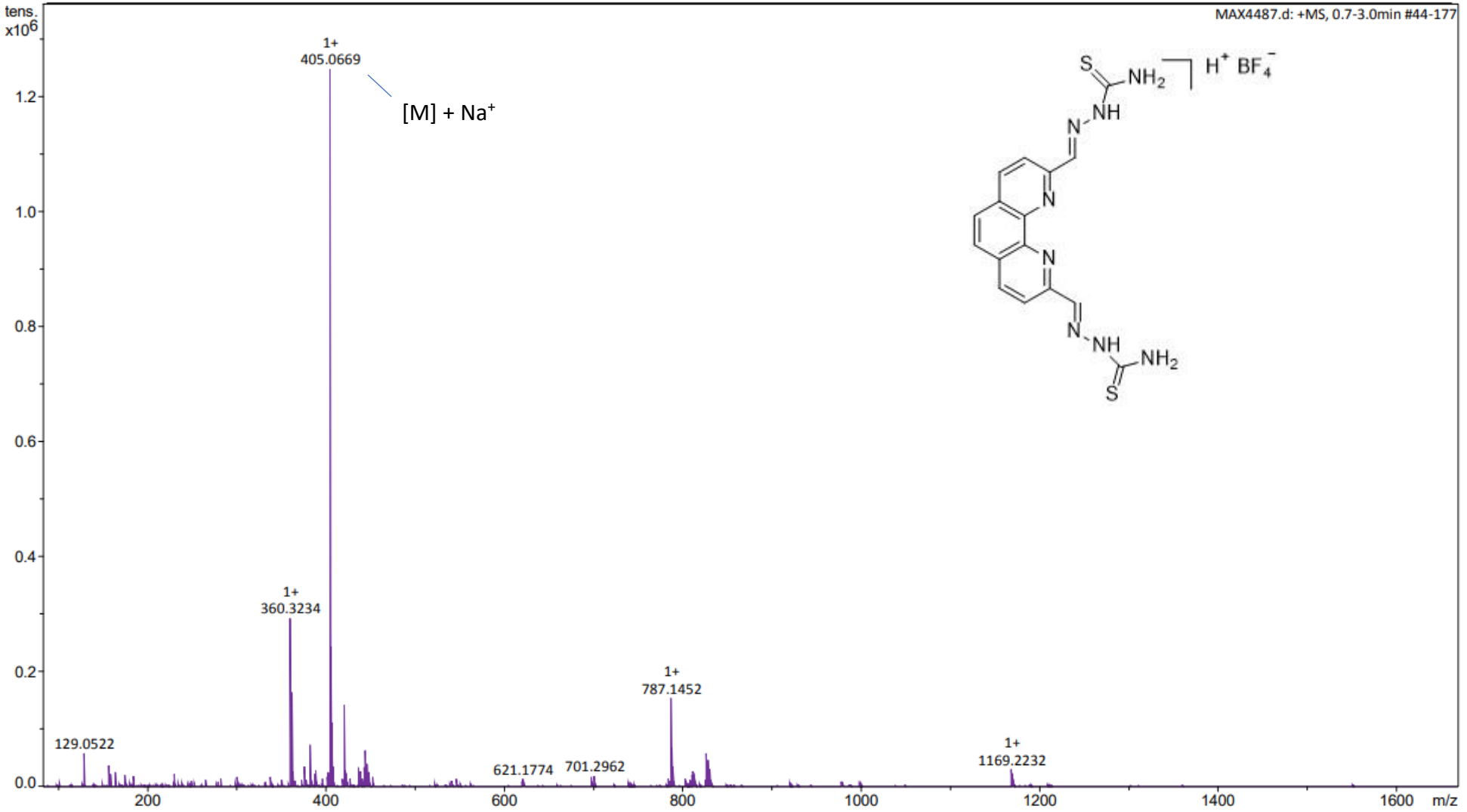

Figure S17. High-resolution electrospray ionization mass spectrum (ESI-HRMS-pos) of **3** (MeOH, 1% formic acid)

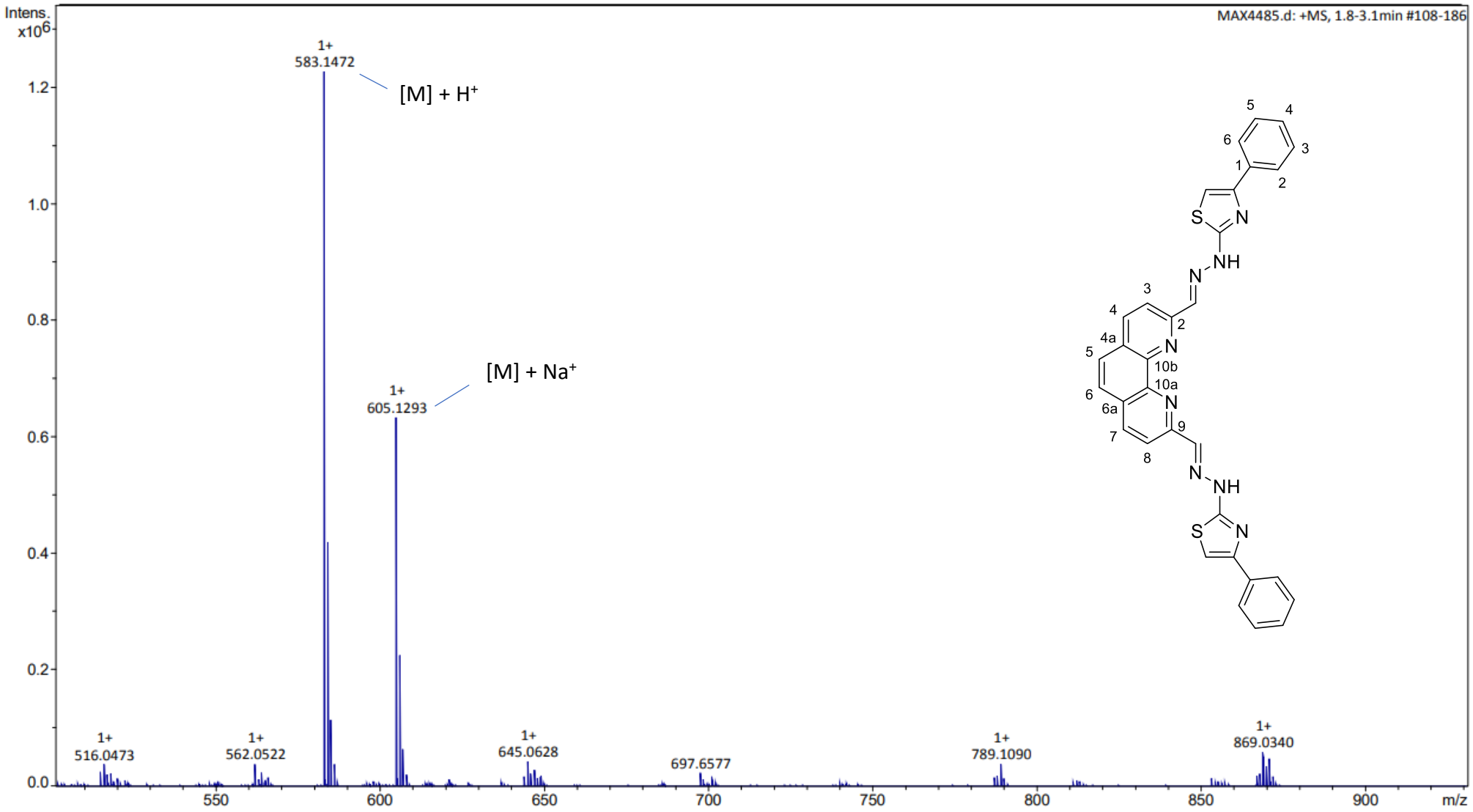

Figure S18. Zoomed view of high-resolution electrospray ionization mass spectrum (ESI-HRMS-pos) of **4** (MeOH, 1% formic acid)

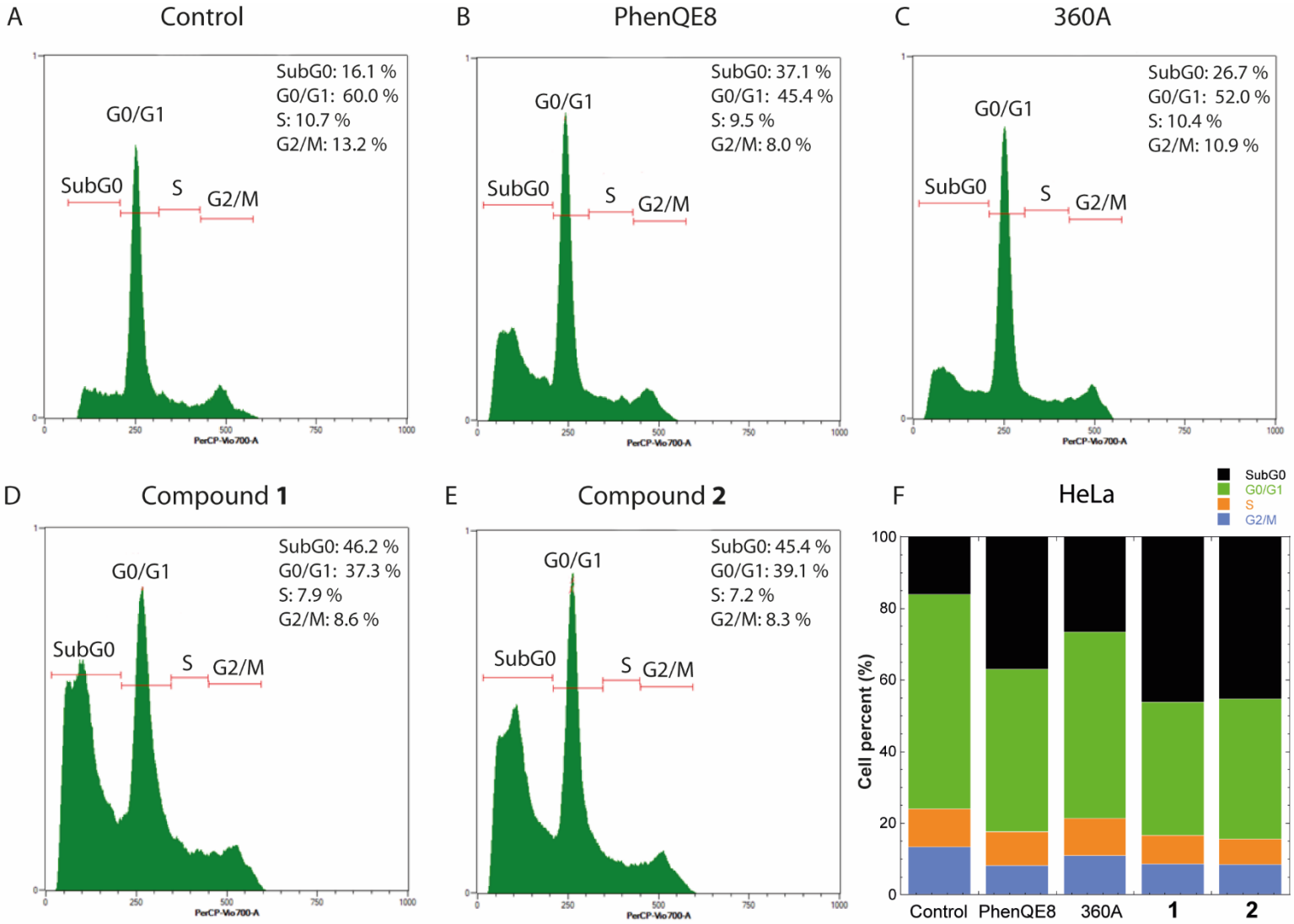

Figure S19. HeLa cell cycle histograms after 72 h treatment with ½ IC_{50} compound concentration. A) Untreated cells (negative control); B) PhenQE8 (structural analogue with antitumor properties, positive control); C) 360A (antitumor agent, positive control); D) compound **1**; E) compound **2**, and F) Stack bar graph representing averaged cell percents in each cycle phase and SubG0 after compound treatment. Increase in the SubG0 population percent is associated to apoptosis.